# Comparison of Monolithic and Partitioned Approaches for the Solution of Fluid-Solid Thermal Interaction Problems

**Emad Tandis**
Faculty of Mechanical Engineering, K. N. Toosi University of Technology, Tehran, Iran
*E.Tandis@email.kntu.ac.ir*

**Ali Ashrafizadeh**
Faculty of Mechanical Engineering, K. N. Toosi University of Technology, Tehran, Iran
*ashrafizadeh@kntu.ac.ir*

## Abstract

*Numerical solution of conjugate heat transfer (CHT) problems in multi-region domains is a challenging issue in terms of efficiency and stability due to inherent coupling between governing equations in separate sub-domains. This paper aims at comparing two distinct strategies for coupling energy equations at interface of regions: partitioned and monolithic. While the former enforces strong coupling via iterative procedures, the latter suggests simultaneous solution of energy equation throughout all regions at once. More precisely, the primary objective of this study is to compare computational costs for three finite volume-based CHT solvers which share a same method for handling pressure-velocity coupling in the fluid, i.e. semi-implicit projection method, and are distinguished from the coupling strategy for energy equation at interface of interacting sub-domains. The first method applies simultaneous solution of energy equation across all regions while second and third ones use separate solver for each region with difference in handling iterative loops. The accuracy and convergence rate of three algorithms are assessed via transient solution of conjugate free convection in fluid and conduction in vertical wall.*

**Key words:** Conjugate heat transfer, monolithic, partitioned, multi-regions, finite volume, convergence rate.

## 1. Introduction

Thermal interaction between fluid flow and solid, known as conjugate heat transfer[1], has been widely studied due to its industrial applications. This problem is classified as a multi-physics phenomenon which is characterized by at least two distinct computational sub-domains, i.e. fluid and solid regions, whose associated equations are coupled at shared boundaries. In addition to interface coupling, there is usually strong coupling between momentum and heat transfer in fluid region which adds more complexity to the CHT problems.

Analysis of this class of multi-physics problems can be carried out in several ways. The first and most straightforward way is analytical method using which one can investigate leading parameters as well as produce results to verify codes. While being accurate enough

[1] CHT

for simple models [1-3], these approaches suffer from restriction to address complex models. Alternatively, experimental methods are more powerful tools for studying practical problems. However, they are usually too expensive and time consuming. Finally, numerical algorithms have yielded tremendous performance in handling variety of the CHT problems [4-6].

Numerical algorithms for CHT problems and multi-physics in general, are usually divided into two classes: partitioned and monolithic. While the former allows for direct use of a specialized solver in each region and consequently offering advantage of code reuse, the latter outperforms in terms of efficiency and stability. In partitioned strategy, fluid and solid solvers are called sequentially [7-10] and accurate enforcement of coupling conditions necessitates a predictor-corrector loop which entails additional computational cost. In contrast, monolithic approach adopts simultaneous solution of identical physics, i.e. energy equation, throughout entire domain to accelerate convergence rate [11, 12].

Appropriate enforcement of coupling conditions at shared interfaces is one of the key effects on accuracy and computational costs in CHT problems especially in unsteady simulations. This has been subject of various researches [13-16] in order to present interface conditions which entail (i) accuracy, (ii) robustness, (iii) less computational cost, (iv) conservation. For instance, Dirichlet–Robin type, whose optimal coupling coefficients has been subject of some studies [15], is frequently suggested for coupling conditions at fluid-solid interface in order to optimize accuracy and robustness of the partitioned algorithms. This coupling condition is based on temperature and heat flux types for fluid and solid, respectively, at shared boundary. Other types of interface coupling, like and Robin–Robin, are investigated in the literature [16] and results are found promising.

Based on the previous studies, two types of coupling play a major role in stability and efficiency of CHT problems: coupling between energy and momentum equations in fluid as well as coupling associated with thermal interaction between two separate regions. In this paper, they are called first and second type, respectively, for simplicity.

This study compares performance of three finite volume-based solvers all of which use a family of semi-implicit projection method[2], i.e. PISO, to handle pressure-velocity coupling. However, they differ in dealing with two types of coupling. In the monolithic approach, PISO algorithm with a single outer iteration is performed for solution of pressure and velocity in all fluid regions and it is followed by simultaneous solution of energy equation across all sub-domains; this procedure, then, continues in a loop till convergence criteria is reached. For partitioned methods, where energy equation for all sub-domains are solved in a sequent way, since one faces two types of coupling, at least two options are available: the first one is to apply separate iterative loop for enforcing each type of coupling, and the second suggests integrating two types of coupling in a single outer loop. Finally, the performance of the three algorithms is assessed via solution of thermal interaction between natural convection in an incompressible flow and conduction in vertical wall. Here, different levels of strength for two types of coupling are considered and results are studied in terms of accuracy and convergence rate.

[2] SIPM

## 2. Governing Equations

This section provides mathematical formulation for a general CHT problem, including governing equations and consistency relations at shared interfaces.

The time dependent equations for describing for a Boussinesq fluid flow- i.e. continuity, momentum and energy equations- are expressed as

$$\nabla.\mathrm{u} = 0 \tag{1}$$

$$\frac{\partial \mathrm{u}}{\partial \mathrm{t}} + \mathrm{u}.\nabla\mathrm{u} = -\nabla\mathrm{p} + \upsilon\nabla^2\mathrm{u} - \mathrm{g}\beta(\mathrm{T} - \mathrm{T}_{\mathrm{ref}}) \tag{2}$$

$$\frac{\partial \mathrm{T}}{\partial \mathrm{t}} + (\mathrm{u}.\nabla)\mathrm{T} = \frac{1}{\rho \mathrm{C}_\mathrm{P}}\nabla.(\mathrm{k}\nabla\mathrm{T}) \tag{3}$$

where u, p, and T are the velocity vector, pressure and temperature of the fluid, respectively, and must be evaluated through solution procedure; g is acceleration vector due to gravity and other parameters denote the fluid properties: ν is the kinematic viscosity, β the thermal expansion coefficient, $C_P$ the heat capacity, k the conductivity and ρ the density of the fluid.

The time dependent energy equation for solid domain is

$$\frac{\partial \mathrm{T_s}}{\partial \mathrm{t}} = \frac{1}{(\rho \mathrm{C_P})_\mathrm{s}}\nabla.(\mathrm{k_s}\nabla\mathrm{T_s}) \tag{4}$$

where subscript s is used to distinguish between solid and fluid parameters. For a well-posed problem, the temperature and heat flux must be continuous at shared interface, $\Gamma_{f,s}$ as follows

$$\mathrm{T}\left(\Gamma_{\mathrm{f,s}}, \mathrm{t}\right) = \mathrm{T_s}\left(\Gamma_{\mathrm{f,s}}, \mathrm{t}\right) \tag{5}$$

$$\nabla.(\mathrm{k}\nabla\mathrm{T}) = \nabla.(\mathrm{k_s}\nabla\mathrm{T_s}) \tag{6}$$

As eqs. (2)-(6) suggest, there are two types of coupling for CHT problem whose strength are function of some non-dimensional quantities. The first refers to coupling between energy and momentum equation in the fluid domain via temperature-velocity coupling. The non-dimensional form of Navier-Stokes for Boussinesq fluid, which is expressed as

$$\frac{\partial \tilde{\mathrm{u}}}{\partial \tilde{\mathrm{t}}} + \tilde{\mathrm{u}}.\nabla\tilde{\mathrm{u}} = -\nabla\tilde{\mathrm{p}} + \frac{1}{\mathrm{Re}^2}\nabla^2\tilde{\mathrm{u}} - \frac{\mathrm{Gr}}{\mathrm{Re}^2}\tilde{\mathrm{T}} \tag{7}$$

$$\frac{\partial \tilde{\mathrm{T}}}{\partial \tilde{\mathrm{t}}} + (\tilde{\mathrm{u}}.\nabla)\tilde{\mathrm{T}} = \frac{1}{\mathrm{RePr}}\nabla^2\tilde{\mathrm{T}} \tag{8}$$

suggests that this coupling highly depends on the Grashof number, $\mathrm{Gr} = \frac{\mathrm{g}\beta(\mathrm{T_H}-\mathrm{T_L})\mathrm{L}^3}{\nu^2}$ and Prandtl number, $\mathrm{Pr} = \frac{\upsilon}{\alpha}$ and Reynolds number, $\mathrm{Re} = \frac{\mathrm{UL}}{\upsilon}$. Therefore, the more Gr is the stronger coupling between momentum and energy equations exists.

The second type of coupling occurs due to continuity of temperature and heat flux at common interface which links energy equations in the fluid and solid regions. The non-dimensional quantity for describing the strength of this coupling is

$$\sigma = \frac{k_f/\sqrt{\alpha_f}}{k_s/\sqrt{\alpha_s}} \tag{9}$$

Here, α is thermal diffusivity. The interaction strength is weak for σ<<1 and increases as σ→1 [12].

## 4. Numerical Approaches

In this section, solution procedure of three CHT solvers are presented each of which apply finite volume method to enforce conservation of physical quantities in all sub-domains as well as at shared interfaces. A same strategy based on the PISO algorithm [17] is used to handle pressure-velocity coupling for fluid regions in all solvers. The solution process starts with discretization of momentum as follows:

$$u_P = \frac{H(u)}{a_P} - \frac{1}{a_P}\nabla p \tag{10}$$

where $a_p$ represents coefficient matrix for each individual cell P, and operator H(u) is evaluated from coefficient matrix for neighbor cells multiplied by their newly calculated velocity plus source term due to buoyancy term. Replacing eq. (10) into (1) leads to pressure equations as below

$$\nabla.\left(\frac{1}{a_p}\nabla p\right) - \nabla.\left[\frac{H(u)}{a_p}\right] = 0 \tag{11}$$

Solution of pressure equation is followed by correcting $u_P$ and flux at faces by eq. (10) and

$$F = \rho s_f.u = \rho s.\left[\left(\frac{H(u)}{a_P}\right)_f - \left(\frac{1}{a_P}\right)_f (\nabla p)_f\right] \tag{12}$$

respectively. The distinguishing aspect of the algorithms is associated with the way of coupling implementation to enforce continuity of temperature and heat flux at shared interfaces, i.e. eqs. (5) and (6), as well as handling momentum-energy coupling for the fluid. Considering the former for partitioned methods, stability of the coupling algorithm highly depends on the correct assignment of boundary conditions for fluid-solid sides of the shared boundary. Therefore, various types of interface condition, which are compared in [15] are suggested for partitioned methods to ensure stability and optimized convergence rate. Henshaw W.D. et al [14] showed that mixed (Robin-Robin) type presents attractive convergence properties especially for the case when adjacent materials have similar properties. In this study, we follow a special implementation of mixed type as suggested in OpenFOAM [18] software based on which each side of interface uses combination of Dirichlet and zero-gradient whose coefficient weights, ω and 1- ω, respectively, are calculated as below:

$$\omega_{own} = \frac{\frac{k_{nei}}{\Delta_{nei}}}{\frac{k_{nei}}{\Delta_{nei}} + \frac{k_{own}}{\Delta_{own}}} \tag{13}$$

Where *own* and *nei* denote both sides of the interface and Δ is perpendicular distance between boundary face and adjacent cell.

For the monolithic solver, simultaneous solution of energy equation throughout all domains requires an appropriate interpolation for conductivity, k, to ensure accurate implementation of energy conservation, i.e. continuity of heat flux, at interface. In the absence of radiation and other source terms at interface, the discretized form of energy conservation is expressed as

$$k_{nei}\frac{(T_{nei}-T_w)}{\Delta_{nei}} = k_{own}\frac{(T_w-T_{own})}{\Delta_{own}} \tag{14}$$

To evaluate k at interface, $k_{int}$, for which well-posed interface condition is ensured, each side of equ. (14) must be identical to $k_{int}\frac{(T_{nei}-T_{own})}{\Delta}$, where Δ is distance between centers of cells at both side of the interface projected on the normal vector of their shared face. This leads to harmonic interpolation of $k_{int}$:

$$k_{int} = \frac{k_f k_s}{\frac{\Delta_f}{\Delta}k_s + \frac{\Delta_s}{\Delta}k_f} \tag{15}$$

For Monolithic solver, the first type of coupling is carried out via an iterative loop. For partitioned methods, which strong coupling for energy equation at interface requires an iterative loop as well, we face two iterative loop for both types of coupling, invoking the question of whether or not integrating them in one general loop is advantageous or not. Fig… illustrates these procedures in more details:

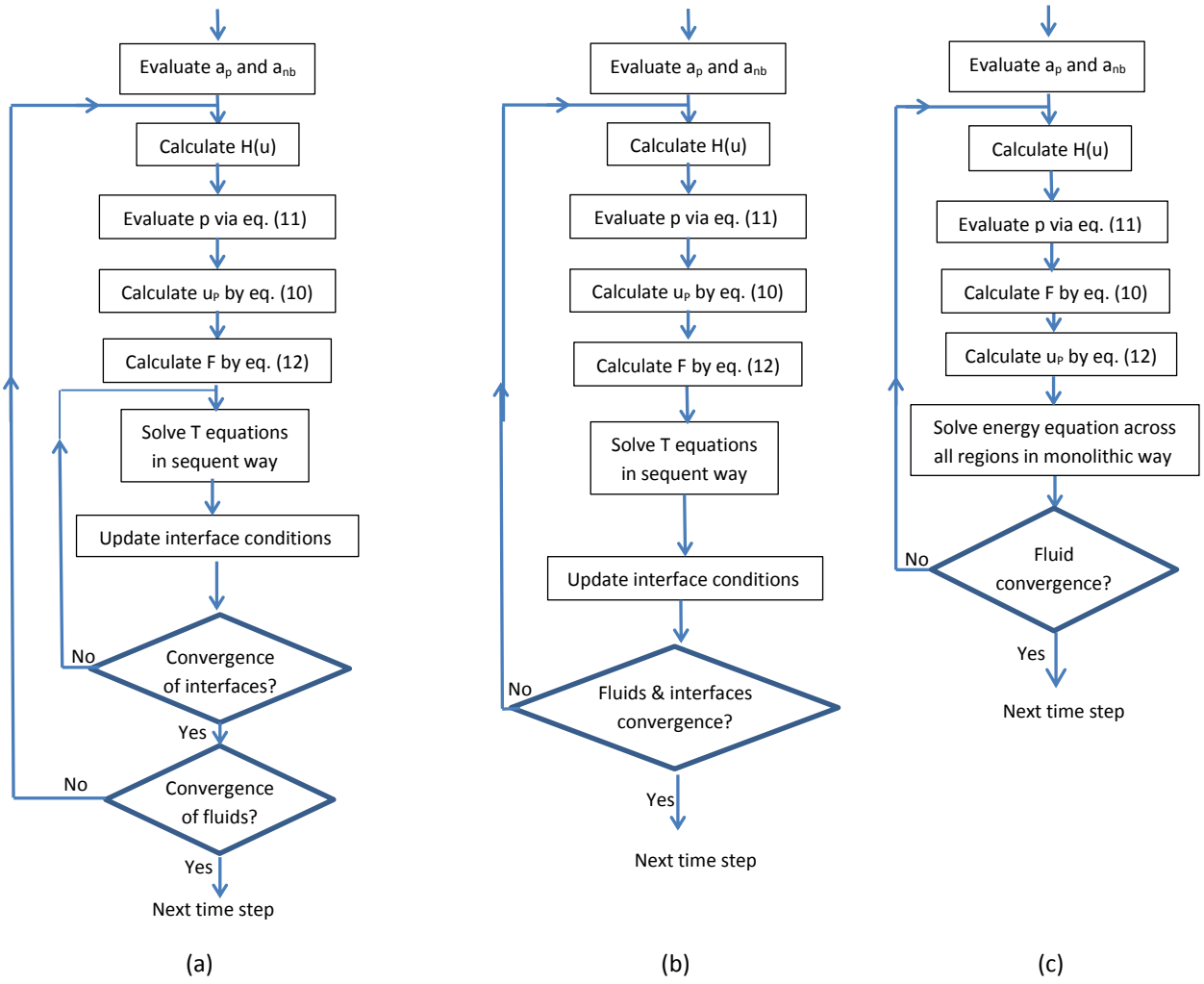


Figure 1- Flowchart of the algorithms of CHT solvers (a) SIPM-SP (b) SIPM-IP (c) SIPM-M

As seen in fig. 1, while algorithm (a), which is called semi-implicit projection method with separate loops (SIPM-SP), suggests an outer iteration for first type of coupling and a sub-

iteration loop for second one, algorithm (b), called semi-implicit projection method with integrated loop (SIPM-IP), integrates two loops into one. However, for monolithic solver, (SIPM-M), as shown in fig. 1 (c), there is only need for one iteration loop to strongly enforce first type of coupling.

We use OpenFOAM software, version of extened4.0, to implement SIPM-M solver, whose prominent feature is simultaneous solution of energy equation in several connected sub-domains, for addressing multi-region CHT problems. In addition, some modifications in another OpenFOAM solver, i.e. chtMultiRegionFoam, is made to simulate CHT problems via SIPM-IP and SIPM-SP.

## 4. Results and Discussion

Numerical results for the case of 2D conjugate natural convection with thermal conduction in a thick vertical wall, shown in fig. 2, are presented to validate the accuracy of solvers.

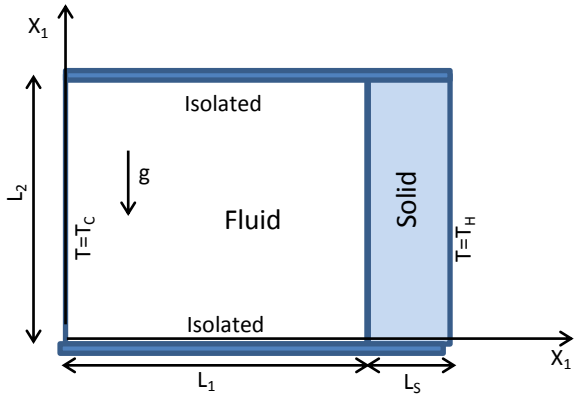


Figure 2- conjugate natural convection with thermal conduction in a thick vertical wall

This case is simulated by many researchers due to its simplicity as well as capability to investigate the effect of two types of coupling via changing some non-dimensional parameters. Among them, Kazemi-Kamyab et al [19] applied a proposed loosely-coupled partitioned algorithm to solve this case in order to demonstrate the applicability of the method for two distinct assumptions: constant material properties and temperature-dependent thermal conductivities in the fluid and solid subdomains. In another study [20], they examined a proposed strongly-coupled partitioned solver through numerical solution of this case for different coupling strength via changing σ and Gr in order to investigate the stability and convergence rate of their algorithm. Also, Pan et al [12] validate accuracy of their proposed monolithic solver through this case for various Gr and σ.

At the present study, we apply three CHT solution algorithms- i.e. SIPM-IP, SIOM-SP and SIPM-M- to validate the results for this case with three types of material properties mentioned in [12]. Table 1 presents non-dimensional number for these states:

Table1. Non-dimensional properties for three cases

| | **Fluid Type** | **Solid Type** | **Pr** | **$k_s/k_f$** | **Gr** | **σ** |
|---|---|---|---|---|---|---|
| Case1 | Air | Steel | 0.7 | 1600 | $1.43\times10^{5}$ | $3.95\times10^{-4}$ |
| Case 2 | Water | Steel | 7 | 80 | $10^{4}$ | 0.12 |
| Case 3 | Water | Concrete | 7 | 2.7 | $10^{4}$ | 0.93 |

In this simulations, we set $L_1/L_2=1$, $L_2=1$and the dimensionless wall thickness $L_S/L_2=0.2$. The fluid is initially at rest with p =0 and T=0. Then it starts to be heated by the heat transferred from the outer surface of the right thick wall with initial temperature of 0 and $T_h=1$, and cooled at the left wall with $T_c=0$ at the same time. The no-slip boundary condition is applied on four walls of the fluid domain. The convergence criteria for interface coupling is $\frac{\max(r^n)}{\max(r^0)}<10^{-6}$ where $r^n$ indicates the interface residual at iteration n. Fig. 3 presents streamlines and contour of temperature in the fluid and solid sub-domains at t=0.07 sec.

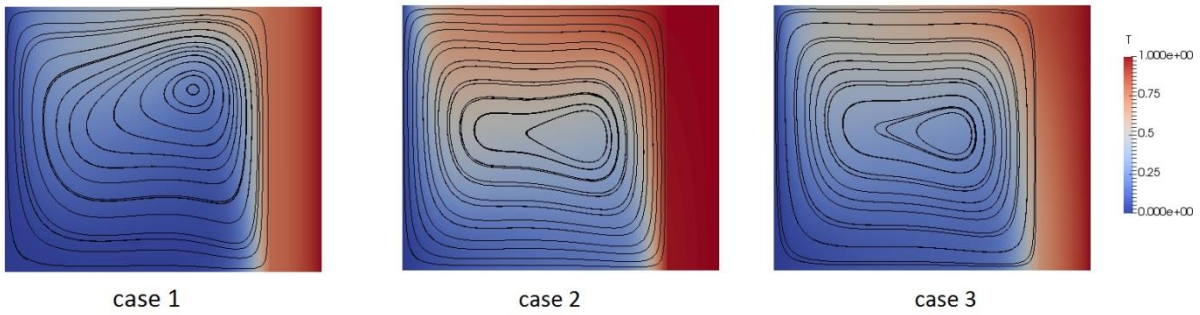


Figure 3- Contour of temperature and streamline for three cases

Fig. 4 compares temperature profile at horizontal midline obtained by proposed solvers with results in [12] for t=0.07 sec. As seen in this figure, three solvers present promising results for case 1, 2 and 3.

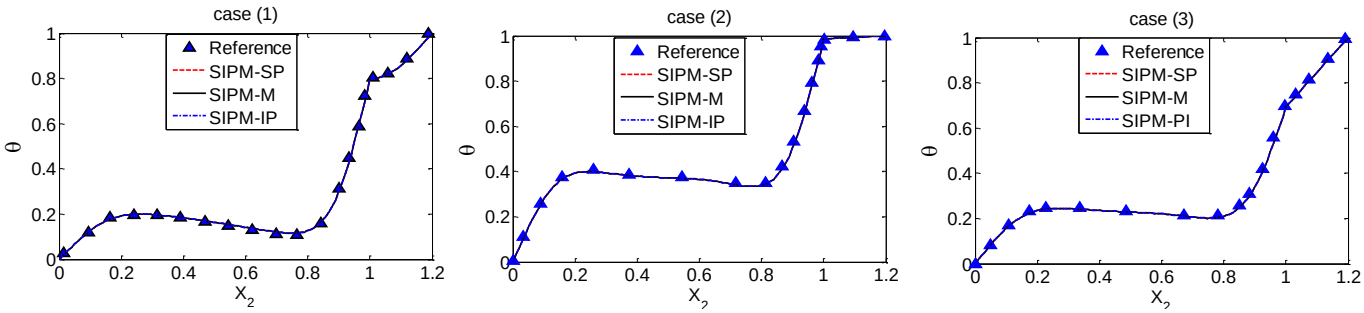


Figure 4- Comparison of temperature profile at $x_2=0.5$ obtained from three solvers with Ref. [12]

For the sake of comparing computational cost of three CHT solvers, we suggest to use new material properties, given in table 2, to provide a situation for comparing solvers at different levels of coupling: strong-strong, strong-weak, weak-strong, and weak-weak- note that the first refers to coupling between momentum and heat transfer in fluid, and second represents thermal coupling between two domains.

Table2. Non-dimensional properties for four cases

| | **Pr** | **$k_s/k_f$** | **Gr** | **σ** |
|---|---|---|---|---|
| CaseA | 0.7 | 1.6 | $1.43\times10^5$ | 0.93 |
| Case B | 0.7 | 1.6 | $10^4$ | 0.93 |
| Case C | 0.7 | 1600 | $1.43\times10^5$ | $4\times10^{-4}$ |
| Case D | 0.7 | 1600 | $10^4$ | $4\times10^{-4}$ |

Computational costs of proposed algorithms for solution of case A to D are compared in fig. 5. As seen in this figure, SIPM-IP produces the slowest convergence rate especially in case A and B, where strong thermal interaction exists between fluid and solid regions. In addition, for case A and B, SIPM-M results in less computational time compared to SIMP-SP. However, as results of case B suggests, this difference tends to reduce when strength of first type coupling decreases due to lower Grashof. Moreover, comparing results of all cases reveals the fact that as the coupling become weak, the computational costs of all algorithms get close to each other.

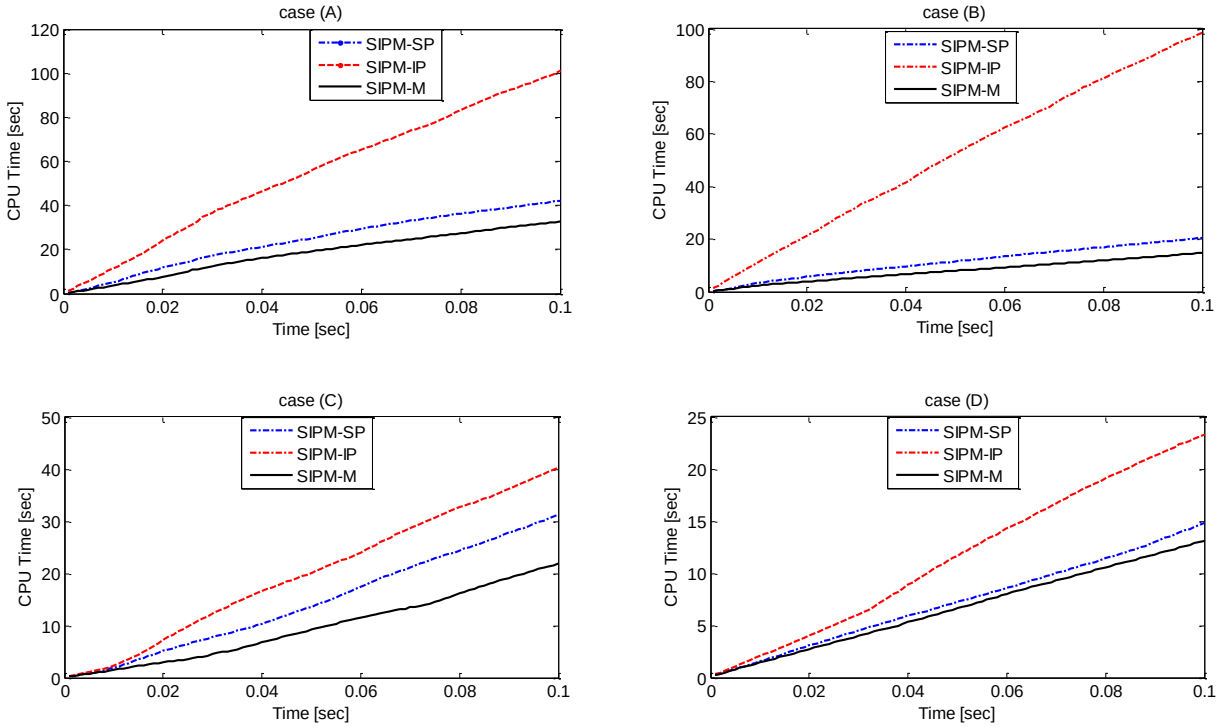


Figure 5- CPU time as a function of solution time for case A to D solver by SIPM-IP, SIPM-SP and SIPM-M solvers

The performance of the solvers is further studied by presenting a new multi-region test case, shown in fig. 6, with parameters given in table 2.

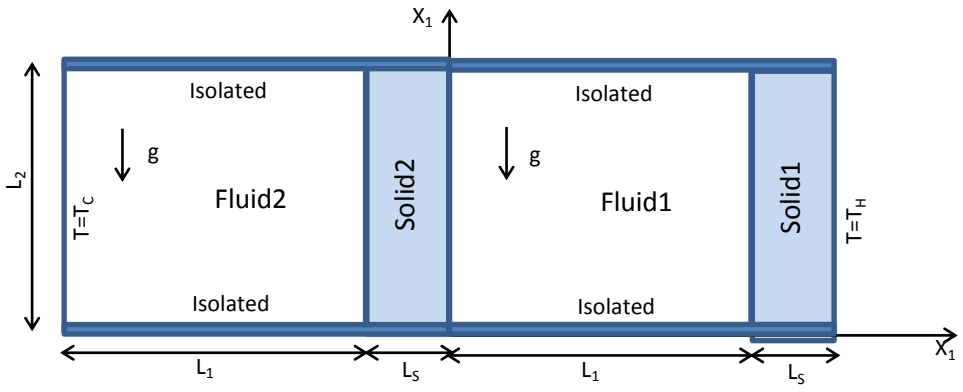


Figure 6- New test case including two regions for solid and two regions for fluid

The main objective of this case is to study performance of the proposed solver when several regions have to be considered in the solution.

The initial state and boundary conditions of this problem is similar to the first case except it consists of two regions for fluid and two regions for solid. This case provides the opportunity to check if increase in number of regions makes a meaningful difference in the convergence rate for considering solvers. Thus, three solvers are used to simulate above problem for case A to D. For case A, velocity contour and streamline are shown in fig. 7.

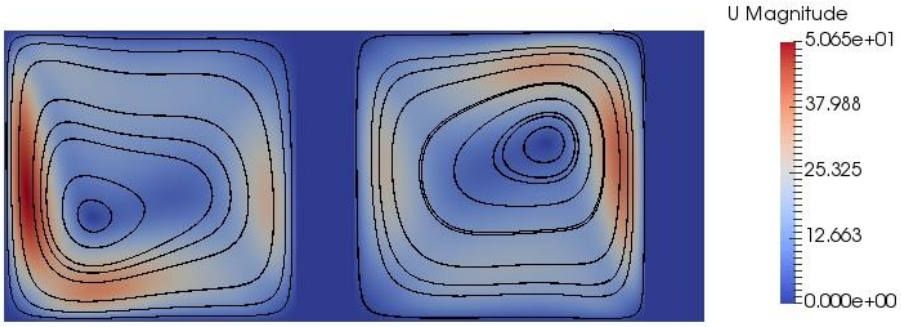


Figure 7- Contour of velocity and streamline for case (A)

In order to ensure accuracy of the discussing algorithms for solution of these cases, variation of the temperature along horizontal midline for case A is shown in fig. 8 based on which it is clear that three algorithms produce nearly identical results for the temperature profile. Since case A possess two types of strong coupling at a same time, and hence more critical to solve, the same procedure for accuracy of other cases is omitted.

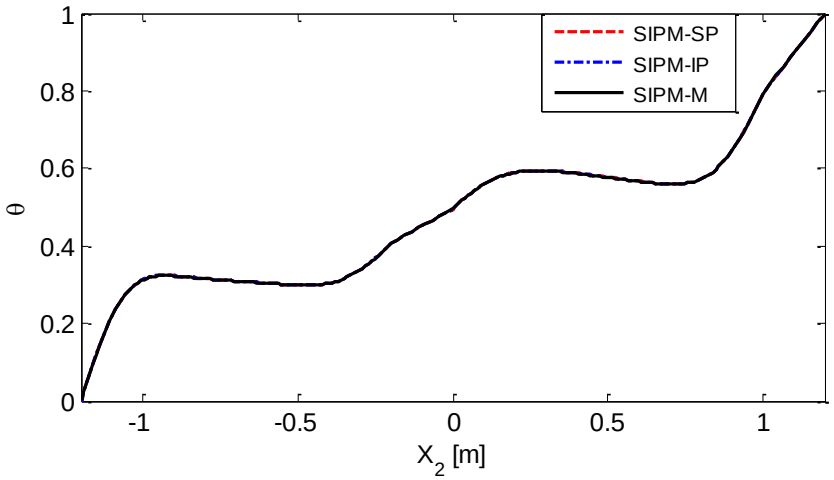


Figure 8- temperature profile at $x_2$=0.5 obtained from three solvers

Fig. 9 compares the CPU time of three solvers for the new problem. As seen, a same behavior, like what was explained in the first test case, is seen. Comparison of the results from fig. 5 and 8 reveals that, for these two problems, three algorithms can be arranged in order of efficiency as: SIPM-M > SIPM-SP > SIPM-IP.

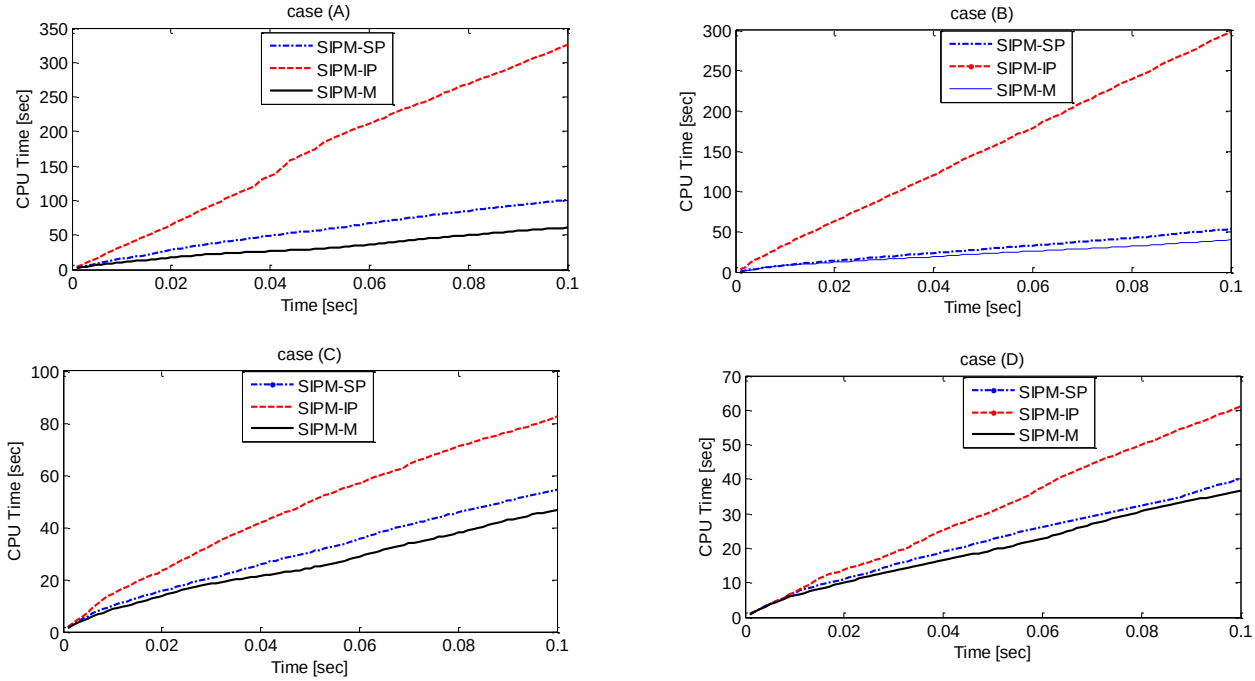


Figure 9- CPU time as a function of solution time for case A to D solver by SIPM-IP, SIPM-SP and SIPM-M solvers

## 5. Conclusions

- Numerical solution of CHT problems requires a special care for coupling of the equations especially when equations are strongly linked to each other.
- Three proposed algorithm are capable of accurately simulate CHT problems.
- Monolithic solution of energy equation across entire domain results in more efficient CHT solver.
- Comparing two types of partitioned methods, i.e. SIPM-IP and SIPM-SP, using separate iterative loop is advantageous in terms of efficiency especially where there is a strong coupling between energy equations at different sub-domains.

.

## References

[1] Pozzi A. and Tognaccini R., 2005, Time singularities in conjugated thermo-fluid-dynamic phenomena, J Fluid Mech, vol. 538, pp 361–76.

[2] Pozzi A. and Tognaccini R., 2000, Coupling of conduction and convection past an impulsively started semi-infinite flat plate. Int J Heat Mass Trans., vol. 43, pp 1121-31.

[3] Fourcher B. and Mansouri K., 1997, An approximate analytical solution to the Graetz problem with periodic inlet temperature, Int J Heat Fluid Flow, vol. 18, pp 229–35.

[4] Ismail K.A.R. and Henriquez J.R., 2005, Two-dimensional model for the double glass naturally ventilated window, Int. J. Heat Mass Transf., vol. 48, pp 461–475.

[5] Gunes H., 2002, Low-order dynamical models of thermal convection in high-aspect ratio enclosures, Fluid Dyn. Res., vol. 30, pp 1–30.

[6] Park S., Lee S., 2015, Analysis of coherent structures in Rayleigh–Bénard convection, J.Turbul., vol. 16, pp 1162–1178.

[7] Moretti R., Errera M. P., Couaillier V. and Feyel F., 2017, Stability, Convergence and Optimization of Interface Treatments in Weak and Strong Thermal Fluid-Structure Interaction, International Journal of Thermal Sciences, vol. 126, pp 23 - 37.

[8] Felippa C.A., Park K.C., 1980, Staggered transient analysis procedures for coupled dynamic systems: formulation, Comput. Methods Appl. Mech. Eng., vol. 24, pp 61-111.

[9] Tallec P. L., 1994, Domain decomposition methods in computational mechanics, Comput. Mech. Adv., vol. 1, pp 220-121.

[10] Piperno S., Farhat C. and Larrouturou B., 1995, Partitioned procedures for the transient solution of coupled aroelastic problems Part I: Model problem, theory and two-dimensional application, Comput. Methods Appl. Mech. Eng., vol. 124, pp 79-112.

[11] Pan X., Kim K., Lee C. and Choi J. I., 2016, A decoupled monolithic projection method for natural convection problems, J.Comput. Phys., vol. 314, pp 160–166.

[12] Pana X., Leea C. and Choi J., 2018, Efficient monolithic projection method for time-dependent conjugate heat transfer problems, Journal of Computational Physics, vol. 369, pp 191–208.

[13] Radenac E., Gressier J. and Millan P., 2014, Methodology of numerical coupling for transient conjugate heat transfer, Computers and Fluids, vol.100, pp 95-107.

[14] Meng F., Banks J.W., Henshaw W.D. and Schwendeman D.W., 2017, A stable and accurate partitioned algorithm for conjugate heat transfer, Journal of Computational Physics, vol. 344, pp 51-85.

[15] Errera M.P. and Duchaine F., 2016, Comparative study of coupling coefficients in Dirichlet–Robin procedure for fluid–structure aerothermal simulations, Journal of Computational Physics, vol. 312, pp 218-234.

[16] Scholl S., Janssens B. and Verstraete R., 2018, Stability of static conjugate heat transfer coupling approaches using Robin interface conditions, Computers & Fluids, vol. 172, pp 209-225.

[17] Issa R.I., 1985, Solution of Implicitly discretized Fluid Flow Equations by Operator-Splitting, Journal of Computational Physics, vol. 62, 40-65.

[18] OpenFOAM project web pages. http://www.openfoam.org, 2004.

[19] Kazemi-Kamyab V., Zuijlen A.H. and Bijl H., 2013, Accuracy and stability analysis of a second-order time-accurate loosely coupled partitioned algorithm for transient conjugate heat transfer problems, Int. J. Numer. Meth. Fluids, DOI: 10.1002/fld.3842.

[20] Kazemi-Kamyab V., Zuijlen A.H. and Bijl H., 2014,. Analysis and application of high order implicit Runge-Kutta schemes for unsteady conjugate heat transfer: A strongly-coupled approach. Journal of Computational Physics, vol. 272, pp 471–486.